IEEE Access
Multidisciplinary Rapid Review Open Access Journal

Received June 29, 2019, accepted July 8, 2019, date of publication July 15, 2019, date of current version August 8, 2019.

Digital Object Identifier 10.1109/ACCESS.2019.2928833

Data-Adaptive Robust Transmission Network Planning Incorporating Post-Contingency Demand Response

QIANWEI ZHENG, XIAOMENG AI, (Member, IEEE), JIAKUN FANG, (Senior Member, IEEE), AND JINYU WEN, (Member, IEEE)

State Key Laboratory of Advanced Electromagnetic Engineering and Technology, School of Electrical and Electronic Engineering, Huazhong University of Science and Technology, Wuhan 430074, China

Corresponding author: Xiaomeng Ai (xiaomengai1986@foxmail.com)

This work was supported in part by the National Natural Science Foundation of China under Grant 51707070 and Grant 51707077, and in part by the China Postdoctoral Science Foundation under Grant M2018642841.

ABSTRACT The significant development and increasing deployment of renewable generation in the modern power system introduces the challenge for dealing with uncertainty. In this paper, data-adaptive robust optimization is applied to the transmission network planning. By taking historical data correlation into account, the proposed model can achieve a lower expansion investment without sacrificing the robustness. Demand response is embedded in this model to relieve the overflow incurred by renewable generation fluctuation and $N-1$ contingency. The model is decomposed into a master problem and several slave problems by column and constraint generation algorithm and then solved iteratively. The numerical simulation tested on Garver 6-bus system and the IEEE 118-bus system demonstrates the effect of demand response in reducing or postponing network construction. The proposed data-adaptive robust optimization is proved to be cost-effective and computationally efficient.

INDEX TERMS Transmission network planning, $N-1$ contingency, demand response, data-adaptive robust optimization, column and constraint generation.

NOMENCLATURE

Parameters

Ω	Set of transmission corridors
$N_{(i)}$	Set of buses connected to bus i
$c_{ij}^{(k)}$	Cost of the kth circuit in transmission corridor (i, j)
$P_{ij}^{(k)\max}$	Maximum power flow along the kth circuit in transmission corridor (i, j)
$x_{ij}^{(k)}$	Reactance of the kth circuit in transmission corridor (i, j)
$n_{ij}^{\max}$	Maximum circuits in transmission corridor (i, j)
$n_{ij}^{\min}$	Number of the existing circuits in transmission corridor (i, j)
$\alpha_{ij}^{(k)*}$	The value of binary variable $\alpha_{ij}^{(k)}$
$P_{Gi}^{\max}/P_{Gi}^{\min}$	Maximum/Minimum conventional power generation at bus i
P_{Di}	Power demand at bus i
P_{Ri}	Renewable energy generation at bus i
$\theta_i^{\max}$	Maximum voltage angle at bus i
v	Ramping rate for conventional units
ΔT	Ramping time for conventional units

Variables

$\alpha_{ij}^{(k)}$	Binary variable regarding the transmission line status of the kth circuit in transmission corridor (i, j)
P_{Gi}/P_{Gi}^{mn}	Conventional power generation at bus i for the normal and post-contingency state
$P_{ij}^{(k)}/P_{ij}^{mn(k)}$	Power flow along the kth circuit in transmission corridor (i, j) for the normal and post-contingency state
P_{ij}/P_{ij}^{mn}	Power flow along transmission corridor (i, j) for the normal and post-contingency state

The associate editor coordinating the review of this manuscript and approving it for publication was Xiaodong Liang.

θ_i/θ_i^{mn}	Voltage angel at bus $\underline{i}$ for the normal and post-contingency state
k_{Di}	Demand response ratio at bus i
PC_{Di}^{mn}	Curtailed power demand of bus i

I. INTRODUCTION

Transmission network expansion planning (TNEP) aims to serve the forecasted demand sufficiently and reliably with minimal investment on the electrical installation during a given planning horizon.

Demand response (DR) has been rapidly developing in recent years as a kind of flexible resource coping with various problems in the power system. A number of DR programs have been implemented worldwide [1]–[3], including some pilot projects and DR potential investigation in China [4], [5]. DR has been employed in both operation [6]–[9] and planning [10]–[13] problems in the power system. For the application in the planning stage, reference [10] utilizes incentive-based demand response as a non-network solution to replace traditional planning method, DR providers will acquire compensation for their contribution to peak load reduction. A multi-objective TNEP model considering customers benefit function and demand price elasticity is proposed in [11]. Reference [12] demonstrates the capacity saving brought by DR in both generation and transmission expansion planning. The effect of DR in economics and locations of transmission investment is investigated in a hybrid AC/DC model in [13]. Both renewable energy generation and DR are taken into account in papers [10]–[13]. However, the capability of DR to handle the power flow violation caused by renewable generation fluctuation is not fully examined. Moreover, the DR benefit in enhancing power system reliability is neglected in these TNEP researches.

On the other hand, with the rapidly increasing deployment of the renewables, various uncertainties are inherently incorporated with TNEP, such as daily fluctuation in load and renewable generation, and occasional policy update [14]–[18]. Plenty of reported attempts have coped with the uncertainties in TNEP, most of which can be generally categorized into stochastic programming or robust optimization.

Stochastic programming characterizes the uncertainties with sampled scenarios from a predefined probability distribution or uncertainty set. However, it is not easy to acquire an accurate distribution of uncertain parameters in practice. Moreover, the solutions obtained by stochastic programming cannot fully satisfy constraints, hence the security cannot be guaranteed.

By contrast, robust optimization calculates with boundary values of uncertainty set to guarantee the system security under all the scenarios in the uncertainty set, so the optimized planning schemes are adaptive to all the situations. The application of robust optimization in TNEP draws broad interests, e.g. [19]–[23]. Reference [19] adopts Benders decomposition (BD) to tackle the uncertainties. The min-max cost and the min-max regret are two kinds of models for robust TNEP problem, their performance is compared for different characteristics of uncertainties in [21]. Reference [20] introduces a tractable adaptive min–max–min cost model to find a robust expansion plan for new lines and storage. In [22], a stochastic adaptive robust optimization is formulated under the centralized planning framework, the investment is optimized in the most suitable generating units among profit-oriented investors. Reference [23] addresses the problem size limitation and computational intractability in dynamic robust TNEP for realistic simulation.

There is still some deficiency remaining in robust optimization for TNEP, one problem lies in the insufficient use of the historical data to characterize the uncertainties. The solution based on the imprecise description of uncertainty like a cubic set is usually over-conservative, because the presence of a worst case in the real world is pretty rare. Some literatures deal with this issue by introducing the "budget of uncertainty" to quantify the degree of conservativeness [24]–[26]. Other researches focus on the combination of stochastic programming and robust optimization [27]–[29]. However, information extraction from historical scenarios is commonly neglected in these approaches.

The conception of data-adaptive robust optimization (DARO) (or distributionally robust [30]) is proposed to fundamentally overcome the over-conservatism. The correlation between historical data is taken into account in this kind of method. Unlike the traditional robust optimization which describes the realization of the uncertain parameters with an interval or polyhedral uncertainty set, DARO shrinks the realization region by utilizing the historical data correlation, and thus reduces the conservativeness [31]. Theories like minimum volume enclosing ellipsoid (MVEE) algorithm [32] and correlation analysis method [33] further demonstrate the effectiveness of DARO. DARO has been applied to tackle with some operation optimization problem in power system [34]–[36]. Reference [30] co-optimizes renewable generation and load reserve with a chance constrained optimal power flow model and solves it with a distributionally robust approach. In [34], a two-stage distributionally robust optimization model is proposed, and the statistical characteristic is considered in a data-driven manner. In [35], a risk-averse stochastic unit commitment problem is solved with a confidence set for the uncertain parameters distributions using statistical inference. Reference [36] applies the data-adaptive robust optimization to the economic dispatch of active distribution networks. Although the effect of DARO is investigated in reducing the operation cost for a power system with uncertain resources, the number of literature incorporating DARO with the TNEP problem is quite limited.

This paper proposes a DAR-TNEP model considering wind power uncertainty and $N-1$ contingency, the contribution can be listed as follows:

1. The uncertainty is tackled with DARO to obtain a less conservative solution and lower planning cost compared to traditional robust optimization. Only a few

scenarios are required to make the decision while the robustness is maintained.

2. The role of DR in this model is to alleviate the overflow incurred by wind power fluctuation and $N-1$ contingency. It can be validated that both DARO and DR help to reduce or postpone the transmission network investment.
3. The model is decomposed with column and constraint generation (C&CG) technique into a master problem and several slave problems. The master problem minimizes the planning investment and slave problems check the post-contingency power flow.

To illustrate the effectiveness of the proposed model, the numerical experiment is conducted on Garver 6-bus system and IEEE 118-bus system.

The remainder of this paper is organized as follows: Section II gives the detailed formulation for the deterministic TNEP problem and uncertainty model with DARO. In Section III, the algorithm structure and solution process of C&CG are described. Simulation results are shown and analyzed in Section IV. Finally, Section V concludes the paper.

II. PROBLEM FORMULATION

In this section, a deterministic TNEP model is proposed. The related transmission network parameters are listed as follows: for branch data, $n_{ij}^{min}/n_{ij}^{\max}$ represents the numbers of existing/maximum circuit between buses i and j, $P_{ij}^{(k)max}$ denotes the capacity of the kth circuit in transmission corridor ij, the cost for one circuit installation in transmission corridor ij is set to $c_{ij}^{(k)}$; for bus data, $P_{Gi}^{\max}/P_{Gi}^{\min}$ represents the maximum/minimum output of the thermal unit at bus i, the ramping rate and duration of the thermal units are set to v and ΔT, respectively the load/wind power output at bus i, $\theta_i^{\max}/\theta_i^{\min}$ limits the upper/lower boundary of phase angle at bus i. The variables in the TNEP model are illustrated as follows: the binary variable $\alpha_{ij}^{(k)}$ determines whether the kth circuit in corridor ij will be installed. If the circuit is installed, $\alpha_{ij}^{(k)}$ takes 1, or 0 otherwise. To distinguish the variables in the normal state and post-contingency state, the superscript mn marks the latter. $P_{ij}^{(k)}/P_{ij}^{(k)mn}$ is defined as the power flow of the kth circuit in transmission corridor ij for the normal/post-contingency state, the total power flow on the corridor for normal/post-contingency state is denoted as P_{ij}/P_{ij}^{mn}, P_{Gi}/P_{Gi}^{mn} and θ_i/θ_i^{mn} refer to the thermal unit output and phase angle at bus i for the normal/post-contingency state.

Price-based demand response (PBDR) and incentive-based demand response (IBDR) are two main types of DR mechanism. Compared to PBDR, IBDR is more schedulable and with faster response. In this paper, IBDR, to be more precise, direct load control is investigated. The model does not optimize demand response cost directly but evaluates the effect of demand response in line investment reduction by the sensitivity analysis of DR ratio, and reasonable demand response cost will be suggested based on the evaluation. Therefore, demand response cost is not included in the objective function which minimizes the line investment, as shown in equation (1):

$$\min \sum_{ij\in\Omega} \sum_{k=n_{ij}^{min}+1}^{n_{ij}^{max}} c_{ij}^{(k)}\alpha_{ij}^{(k)} \tag{1}$$

A. DETERMINISTIC TNEP PROBLEM

1) BASE CASE CONSTRAINTS

The constraints under the normal state can be formulated as follows:

$$\alpha_{ij}^{(k)} \in \{0, 1\} \quad k = n_{ij}^{min}+1, \ldots, n_{ij}^{max} \tag{2}$$

$$\alpha_{ij}^{(k)} = 1k = 1, \ldots, n_{ij}^{min} \tag{3}$$

$$\alpha_{ij}^{(k)} \leq \alpha_{ij}^{(k-1)}k = 2, \ldots, n_{ij}^{max} \tag{4}$$

$$n_{ij}^{min} \leq \sum_{k=1}^{n_j^{max}} \alpha_{ij}^{(k)} \leq n_{ij}^{max} \tag{5}$$

$$P_{Gi} + P_{Ri} - P_{Di} = \sum_{j\in N(i)} P_{ij} \tag{6}$$

$$P_{ij} = \sum_{k=1}^{n_{ij}^{max}} P_{ij}^{(k)} \tag{7}$$

$$\begin{aligned} -2\theta^{max}\left(1-\alpha_{ij}^{(k)}\right) &\leq \theta_i - \theta_j - x_{ij}^{(k)}P_{ij}^{(k)} \\ &\leq 2\theta^{max}\left(1-\alpha_{ij}^{(k)}\right) \end{aligned} \tag{8}$$

$$-P_{ij}^{(k)max}\alpha_{ij}^{(k)} \leq P_{ij}^{(k)} \leq P_{ij}^{(k)max}\alpha_{ij}^{(k)} \tag{9}$$

$$P_{Gi}^{min} \leq P_{Gi} \leq P_{Gi}^{max} \tag{10}$$

$$-\theta^{max} \leq \theta_i \leq \theta^{max} \tag{11}$$

Constraints (2)-(3) enforce the values of binary variable $\alpha_{ij}^{(k)}$ for the candidate/existing circuits. Constraint (4) limits the sequential installation of circuits in each transmission corridor. Constraint (5) restricts the maximum and minimum circuits in corridor ij. Constraint (6) reflects the power balance at each bus. Constraint (7) shows the addition of power flow on all the circuits in each corridor. Constraint (8) enforces the relationship between circuit power flow and phase angles at the ends of circuits. Constraints (9)-(11) restrict the upper and lower limits for the circuit power flow/generator output/phase angle.

2) POST-CONTINGENCY CONSTRAINTS BASED ON DR MECHANISM

$$\alpha_{ij}^{(K)} = 0 \quad K = n_{ij}^{min} \tag{12}$$

$$\alpha_{ij}^{(k)} = 1 \quad k = 1, \ldots, n_{ij}^{min}-1 \tag{13}$$

$$P_{Gi}^{mn} + P_{Ri} - (P_{Di} - PC_{Di}^{mn}) = \sum_{j\in N(i)} P_{ij}^{mn} \tag{14}$$

$$P_{ij}^{mn} = \sum_{k=1}^{n_{ij}^{max}} P_{ij}^{mn(k)} \tag{15}$$

$$-2\theta^{max}\left(1-\alpha_{ij}^{(k)}\right) \leq \theta_i^{mn} - \theta_j^{mn} - x_{ij}^{(k)} P_{ij}^{mn(k)} \leq 2\theta^{max}\left(1-\alpha_{ij}^{(k)}\right) \tag{16}$$

$$-P_{ij}^{(k)max}\alpha_{ij}^{(k)} \leq P_{ij}^{mn(k)} \leq P_{ij}^{(k)max}\alpha_{ij}^{(k)} \tag{17}$$

$$P_{Gi}^{min} \leq P_{Gi}^{mn} \leq P_{Gi}^{max} \tag{18}$$

$$-\theta^{max} \leq \theta_i^{mn} \leq \theta^{max} \tag{19}$$

$$0 \leq PC_{Di}^{mn} \leq k_{Di} \cdot P_{Di} \tag{20}$$

$$-v\Delta T \leq P_{Gi}^{mn} - P_{Gi} \leq v\Delta T \tag{21}$$

Constraint (12) enforces the value of $\alpha_{ij}^{(k)}$ for the Kth ($K = n_{ij}^{min}$) circuit in corridor ij to be 0 after it's removed for contingency. The values of $\alpha_{ij}^{(k)}$ for other existing circuits remain 1, as shown in constraint (13). Constraint (14) is the post-contingency power balance constraint considering demand response. Constraints (15)-(16) show the post-contingency total corridor power flow formulation and power flow-phase angle relation, respectively. Constraints (17)-(19) enforce the upper and lower limits for post-contingency circuit power flow/generator output/phase angle. Constraint (20) indicates the load shedding in the post-contingency case. The DR ratio k_{Di} determines the maximum load that can respond to $N-1$ contingency and wind power output fluctuation. Different k_{Di} can be set for different load buses. Constraint (21) indicates the generator output re-dispatch after $N-1$ contingency. It's noteworthy that constraints (6)-(8) and constraints (14)-(16) formulate the power flow constraints without the sensitivity matrix between power injection at buses and power flow on circuits, the disjunctive manner enables the TNEP model to be linear [16].

B. PROBLEM REFORMATION

The proposed TNEP model can be formulated in the general compact form as follow:

$$\min F = c(x)$$
$$s.t. \begin{cases} f_1(x) = 0 \\ f_2(x) \geq 0 \\ g_1\left(\mathbf{p}_w, x, y^b\right) = 0 \\ g_2\left(\mathbf{p}_w, x, y^b\right) \geq 0 \\ h_1\left(\mathbf{p}_w, x, y^c\right) = 0 \\ h_2\left(\mathbf{p}_w, x, y^c\right) \geq 0 \end{cases} \tag{22}$$

where $\boldsymbol{p}_w$ is the stochastic wind power output; x is corresponding to the binary variable $\alpha_{ij}^{(k)}$ to determine whether the candidate transmission line to be installed or not; y^b and y^c refer to the operation-related, continuous variables (e.g. generator output and power flow) in the normal state and $N-1$ contingency, respectively. $c(x)$ is the objective of line investment which is only decided by x. The constraints $f_1(x) = 0/f_2(x) \geq 0$ include problem (2)-(5) and (12)-(13). The constraints $g_1\left(\boldsymbol{p}_w, x, y^b\right) = 0/g_2\left(\boldsymbol{p}_w, x, y^b\right) \geq 0$ represent the base case constraints (6)-(11), while the constraints $h_1\left(\boldsymbol{p}_w, x, y^b\right) = 0/h_2\left(\boldsymbol{p}_w, x, y^b\right) \geq 0$ represent the post-contingency constraints (14)-(21). Therefore, the proposed model is a stochastic mixed integer linear programming (MILP) model.

To tackle the uncertainty of renewable energy generation, DARO is adopted here, using the improved two-stage robust optimization (TRO). The first stage determines the values of integer variables, while the second stage solves the remaining linear problem with the certain values of integer variables. In the second stage, extreme scenarios are used to verify the effectiveness of the solution in multiple situations. These extreme scenarios are selected using MVEE and correlation analysis method. With this means, the number of extreme scenarios is considerably reduced. Hence, the computational burden can be relieved, meanwhile the system security can be guaranteed [19].

For the extreme scenarios of n wind farms, if n set of y^b and y^c that individually adapt to each wind power output scenario are available for the planning scheme x, then x accommodates all the wind power output scenarios. Optimization (22) can be transformed into (23) and $\tilde{\boldsymbol{p}}_{we,i}$ denotes the ith extreme scenario of wind power output:

$$\min F = c(x)$$
$$s.t. \begin{cases} f_1(x) = 0 \\ f_2(x) \geq 0 \\ g_1(\widetilde{p}_{we,i}, x, y_i^b) = 0 & i = 1, \ldots, N_e \\ g_2(\widetilde{p}_{we,i}, x, y_i^b) \geq 0 & i = 1, \ldots, N_e \\ h_1(\widetilde{p}_{we,i}, x, y_i^c) = 0 & i = 1, \ldots, N_e \\ h_2(\widetilde{p}_{we,i}, x, y_i^c) \geq 0 & i = 1, \ldots, N_e \end{cases} \tag{23}$$

Therefore, a planning scheme satisfying the extreme scenarios of wind power output can adapt to all the wind power output scenarios. The robustness of power system is guaranteed. The proposed model is reformed into a DAR-TNEP model.

III. SOLUTION TECHNIQUE

The data-adaptive extreme scenario method can markedly relieve the computational burden by limiting the wind power output scenarios. However, $N-1$ contingency is another challenge for reducing the solving time, especially when the model is applied to a large-scale system. A column-constraint generation (C&CG) method is applied to solve the MILP problem and enhance computational performance.

A. COLUMN-AND-CONSTRATINT GENERATION (C&CG)

The C&CG method decomposes the primal problem into a master problem and several sub-problems.

1) MASTER PROBLEM: INVESTMENT OPTIMIZATION

The master problem is a TNEP problem that decides the planning scheme by solving problem (24) with the worst scenario $\tilde{\boldsymbol{p}}_{we,s}$ identified in sub-problems.

$$\min F_{mas} = \eta + c(x)$$
$$s.t. \begin{cases} f_1(x) = 0 \\ f_2(x) \geq 0 \\ g_1(\widetilde{\mathbf{p}}_{we,s}, x, y_s^b) = 0 & s = 1, \ldots, n \\ g_2'(\widetilde{\mathbf{p}}_{we,s}, x, y_s^b) \geq 0 & s = 1, \ldots, n \\ g_2''(\widetilde{\mathbf{p}}_{we,s}, x, y_s^b) \geq R_s^b & s = 1, \ldots, n \\ h_1(\widetilde{\mathbf{p}}_{we,s}, x, y_s^c) = 0 & s = 1, \ldots, n \\ h_2'(\widetilde{\mathbf{p}}_{we,s}, x, y_s^c) \geq 0 & s = 1, \ldots, n \\ h_2''(\widetilde{\mathbf{p}}_{we,s}, x, y_s^c) \geq R_s^c & s = 1, \ldots, n \\ \eta \geq \sum\limits_{ij \in \Omega} \sum\limits_{k=1}^{n_{ij}^{\max}} (s_{1,ij}^{(k)} + r_{1,ij}^{(k)} + s_{2,ij}^{(k)} + r_{2,ij}^{(k)} \\ +s_{3,ij}^{(k)} + r_{3,ij}^{(k)} + s_{4,ij}^{(k)} + r_{4,ij}^{(k)}) \end{cases} \tag{24}$$

2) SUB-PROBLEMS: OVERFLOW CHECK FOR EVERY EXTREME SCENARIO

The planning scheme derived in the master problem is denoted by $\alpha_{ij}^{(k)*}$ (namely every circuit in transmission corridor ij is determined). The sub-problems will be solved with $\alpha_{ij}^{(k)*}$ to check whether any overflow will occur due to extreme wind power output or $N-1$ contingency. If any overflow occurs in sub-problems, the worst scenario corresponding to the maximal overflow will be found. A set of constraints for the worst scenario are generated and added to the master problem. Then the master problem is solved in the next iteration and update the planning scheme $\alpha_{ij}^{(k)*}$.

With the variable $\alpha_{ij}^{(k)}$ fixed to $\alpha_{ij}^{(k)*}$, the sub-problems become line programming (LP) problems. Every sub-problem is solved for a specific extreme scenario, so the number of sub-problem N_e equals to the number of extreme scenarios. Both the base case constraints (6)-(11) and the post-contingency case constraints (12)-(21) are included in a sub-problem where P_{Ri} and $\alpha_{ij}^{(k)}$ are substituted by $\tilde{\boldsymbol{p}}_{we,i}$ and $\alpha_{ij}^{(k)*}$.

To ensure the feasibility for sub-problems, non-negative slack variables $s_{1,ij}^{(k)}, r_{1,ij}^{(k)}, s_{2,ij}^{(k)}, r_{2,ij}^{(k)}$ (represented by R_s^b) and $s_{3,ij}^{(k)}, r_{3,ij}^{(k)}, s_{4,ij}^{(k)}, r_{4,ij}^{(k)}$ (represented by R_s^c) are added to the power flow formulations for base case ($g_2'' \geq R_s^b$) and post-contingency case ($h_2'' \geq R_s^c$), respectively. The specific constraints are shown by (25)-(28).

$$\begin{aligned} P_{ij}^{(k)} - s_{1,ij}^{(k)} &\leq P_{ij}^{(k)max} \alpha_{ij}^{(k)*} \\ -P_{ij}^{(k)} - r_{1,ij}^{(k)} &\leq P_{ij}^{(k)max} \alpha_{ij}^{(k)*} \end{aligned} \tag{25}$$

$$\begin{aligned} \theta_i - \theta_j - x_{ij}^{(k)} P_{ij}^{(k)} - s_{2,ij}^{(k)} &\leq 2\theta^{max} \left(1 - \alpha_{ij}^{(k)*}\right) \\ -(\theta_i - \theta_j - x_{ij}^{(k)} P_{ij}^{(k)}) - r_{2,ij}^{(k)} &\leq 2\theta^{max} \left(1 - \alpha_{ij}^{(k)*}\right) \end{aligned} \tag{26}$$

$$\begin{aligned} P_{ij}^{mn(k)} - s_{3,ij}^{(k)} &\leq P_{ij}^{(k)max} \alpha_{ij}^{(k)*} \\ -P_{ij}^{mn(k)} - r_{3,ij}^{(k)} &\leq P_{ij}^{(k)max} \alpha_{ij}^{(k)*} \end{aligned} \tag{27}$$

$$\begin{aligned} \theta_i^{mn} - \theta_j^{mn} - x_{ij}^{(k)} P_{ij}^{mn(k)} - s_{4,ij}^{(k)} &\leq 2\theta^{max} \left(1 - \alpha_{ij}^{(k)*}\right) \\ -(\theta_i^{mn} - \theta_j^{mn} - x_{ij}^{(k)} P_{ij}^{mn(k)}) - r_{4,ij}^{(k)} &\leq 2\theta^{max} \left(1 - \alpha_{ij}^{(k)*}\right) \end{aligned} \tag{28}$$

The sub-problems can be formulated by (29):

$$\min F_{sub} = \eta + c(x^*)$$
$$s.t. \begin{cases} g_1(\widetilde{\mathbf{p}}_{we,s}, x^*, y_s^b) = 0 \\ \quad s = 1, \ldots, N_e \\ g_2'(\widetilde{\mathbf{p}}_{we,s}, x^*, y_s^b) \geq 0 \\ \quad s = 1, \ldots, N_e \\ g_2''(\widetilde{\mathbf{p}}_{we,s}, x^*, y_s^b) \geq R_s^b \\ \quad s = 1, \ldots, N_e \\ h_1(\widetilde{\mathbf{p}}_{we,s}, x^*, y_s^k) = 0 \\ \quad s = 1, \ldots, N_e \\ h_2'(\widetilde{\mathbf{p}}_{we,s}, x^*, y_s^k) \geq 0 \\ \quad s = 1, \ldots, N_e \\ h_2''(\widetilde{\mathbf{p}}_{we,s}, x^*, y_s^k) \geq R_s^c \\ \quad s = 1, \ldots, N_e \\ \eta \geq \sum\limits_{ij \in \Omega} \sum\limits_{k=1}^{n_{ij}^{\max}} (s_{1,ij}^{(k)} + r_{1,ij}^{(k)} + s_{2,ij}^{(k)} + r_{2,ij}^{(k)} \\ +s_{3,ij}^{(k)} + r_{3,ij}^{(k)} + s_{4,ij}^{(k)} + r_{4,ij}^{(k)}) \end{cases} \tag{29}$$

The values of F_{mas} and F_{sub} are the low bound (LB) and upper bound (UB) of the objective function in the primal problem, respectively. LB gets higher and UB gets lower with the iterations. When $UB = LB$, the iteration is terminated and the optimal planning scheme is generated.

B. SUMMARY OF THE SOLUTION PROCEDURE

The procedure of the solution method is as follows:

Step 1): Input system parameters and wind power profiles;

Step 2): Generate data-adaptive extreme scenarios.

Step 3): Set $LB = -\infty$, $UB = +\infty$;

Step 4): Solve the sub-problems with the original transmission network for the first iteration or $\alpha_{ij}^{(k)*}$ for the next iterations, identify the worst scenario and generate appropriate constraints, update UB;

Step 5): Solve the master problem with constraints for the worst scenario generated in Step 4, update $\alpha_{ij}^{(k)*}$ and LB;

Step 6): If $|UB - LB| \leq \varepsilon$, terminate the iteration and list the optimal planning scheme, otherwise repeat Step 4 to 5.

IV. NUMERICAL RESULTS

The Garver 6-bus system and IEEE 118-bus system are simulated in this section to validate the effectiveness of the proposed method. The experiment is performed on a personal computer with Intel Core^{TM}i5-6200U CPU (2.3GHz) and 8GB of memory, using Matlab 2014b and Gurobi 7.0.2 as the solver.

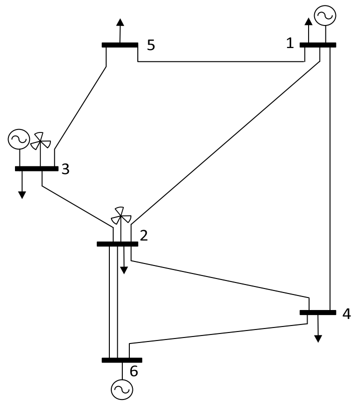

FIGURE 1. Electric diagram of Garver six-bus system.

TABLE 1. Cost of the stochastic case with different DR ratios for Garver 6-bus system (TR-TNEP).

DR ratio	Maximal DR response (MW)	LIC (10^6 \$)	DFC (10^6 \$)	DIC (10^6 \$)	TC (10^6 \$)
0	0	420	0	0	420
2%	28.8	400	0.88	0.09	400.97
4%	57.6	400	1.77	0.18	401.95
6%	81.6	400	2.65	0.25	402.90
8%	102	380	3.53	0.31	383.84
10%	136	340	4.41	0.42	344.83

A. GARVER 6-BUS SYSTEM

Fig.1 shows the topology of the Garver 6-bus system that consists of 3 thermal units with 2340 MW installed, five load buses of 1440 MW and 9 transmission lines. The generator ramp rate is assumed as 1% of the maximum output. The emergency re-dispatch time after $N-1$ contingency is set to 10min. Two wind farms are installed at Bus 2 and Bus 3, respectively. The extreme scenarios generated by TR-TNEP or DAR-TNEP are shown in TABLE 9 and in TABLE 10 in the Appendix.

The transmission line installation cost (LIC) takes the practical experiences from Chinese TSO as reference. The investment in DR aspect is considered as two parts of facility investment (DFC, 30.65 k\$/MW) and incentive pay for circuit fault (DIC, 3.065 k\$/MW once). The former is proportional to the available maximum demand response, while the latter relates to the actual maximum load curtailment in all the $N-1$ contingencies considered. DR ratios at all the load buses are set identically.

1) THE INFLUENCE OF DR RATIO ON THE TOTAL COST

In this section, the effects of DR to reduce the total investment of TNEP will be investigated. The uncertainty of wind power is only characterized by TR-TNEP. The cost for different DR ratios is shown in TABLE 1, where maximal DR response refers to the sum of overflow occurs in all the contingency.

It is indicated by the results of 0, 2%, 8% and 10% DR ratios that DR acts as an alternative for transmission line expansion to achieve a lower total cost. However, the DR ratios of 4% and 6% make no difference in line investment, which results in a higher total cost for a larger DR ratio due to more DR investment. The inherent reason lies in that the decision variables for circuits are not continuous, but discrete. An identical planning scheme can be obtained for similar DR ratios. Therefore, to reduce line investment and total cost in an effective way, a proper DR ratio should be chosen carefully based on the feature of the considered power system.

To further investigate the issue, all the extreme scenarios are examined individually for different DR ratios, the detailed line investment is listed in TABLE 2, where ES is the short for extreme scenario

TABLE 2. Comparison between the transmission line investments cost in the stochastic case and all certain cases for Garver 6-bus system.

DR ratio	Stochastic Case (10^6 \$)	Single extreme scenario (10^6 \$)			
		ES1	ES2	ES3	ES4
0	420	420	360	240	240
2%	400	400	360	240	240
4%	400	400	360	240	240
6%	400	360	320	240	240
8%	380	360	320	240	240
10%	340	340	320	240	240

For the results considering the DR ratios less than 6%, the line investment in the uncertain case is almost determined by ES1 (when both of the two wind farms give the minimum output). Additionally, the uncertain case provides costlier planning schemes than any single extreme scenario when the DR ratio is 6%. The line investment in the uncertain case is a comprehension decision rather than just a copy of that in a single scenario. Therefore, planning schemes achieved by any one extreme scenario may not satisfy the demand for wind power uncertainty, i.e., it's necessary to consider wind power uncertainty.

2) THE INFLUENCE OF DR DISTRIBUTION

In practical situations, electricity consumers are usually categorized into several priority levels when they are engaged in the DR programs, according to they are industrial loads or commercial users. Therefore, different DR ratios may be set for loads with different importance. A lower total cost of TNEP can be achieved by assigning the DR resource properly. Here we divide the whole load in the six-bus system into two parts evenly (P_{D1}, P_{D2}, P_{D3} and P_{D4}, P_{D5}, P_{D6}) and only one part takes part in DR program. The results shown in TABLE 3 indicates an evident reduction in line investment when DR ratios take 20%. In this case, if DR programs are performed on Bus 4-6, the wind power at Bus 2 and Bus 3 will be consumed by the more local load, which saves some costlier circuits to transform the resource.

TABLE 3. Results of the stochastic case with different DR distribution (TR-TNEP).

DR distribution	Maximal DR ratio = 0	Maximal DR ratio = 10%		Maximal DR ratio = 20%	
	k_{Di} = [0;0;0;0;0;0]	k_{Di} =[0.1;0.1;0.1;0;0;0]	k_{Di} = [0;0;0;0.1;0.1;0.1]	k_{Di} = [0.2;0.2;0.2;0;0;0]	k_{Di} = [0;0;0;0.2;0.2;0.2]
Maximal DR response(MW)	0	64	72	144	144
LIC(10^6 \$)	420	400	400	360	320
DFC(10^6 \$)	0	2.20	2.20	4.41	4.41
DIC(10^6 \$)	0	0.20	0.22	0.44	0.44
TC(10^6 \$)	420	402.40	402.42	364.85	324.85

TABLE 4. Results of the stochastic case with different DR ratios for Garver 6-bus system (DAR-TNEP).

DR ratio	Maximal DR response (MW)	LIC (10^6 \$)	DFC (10^6 \$)	DIC (10^6 \$)	TC (10^6 \$)
0	0	380	0	0	380
2%	28.8	380	0.88	0.09	380.97
4%	57.6	360	1.77	0.18	361.95
6%	81.6	320	2.65	0.25	322.90
8%	115	320	3.53	0.35	323.88
10%	144	320	4.41	0.44	324.85

TABLE 5. The transmission line investment reduction by unit DR for the cases under different DR ratios.

DR ratio	TR-TNEP (10^6 \$/MW)	DAR-TNEP (10^6 \$/MW)
2%	0.69	0
4%	0.35	0.35
6%	0.23	0.69
8%	0.35	0.52
10%	0.42	0.42

TABLE 6. Results of the stochastic case with different DR ratios for IEEE 118-bus system (TR-TNEP).

DR ratio	Maximal DR response (MW)	LIC (10^6 \$)	DFC (10^6 \$)	DIC (10^6 \$)	TC (10^6 \$)
0	0	742	0	0	742
10%	265.4	710	26	0.81	736.81
20%	546.4	698	52	1.68	751.68

3) COMPARISON BETWEEN TR-TNEP AND DAR-TNEP

The cost with the application of DAR-TNEP is given in TABLE 4.

Compared with the TR-TNEP results in TABLE 1, the proposed DAR-TNEP method can offer a more economical investment for all the DR ratios considered. However, whether the DR program would effectively reduce the total cost also depends on a reasonable DR ratio.

TABLE 7. Results of the stochastic case with different DR ratios for IEEE 118-bus system (DAR-TNEP).

DR ratio	Maximal DR response (MW)	LIC (10^6 \$)	DFC (10^6 \$)	DIC (10^6 \$)	TC (10^6 \$)
0	0	476	0	0	476
10%	258.6	444	26	0.79	470.79
20%	566.4	432	52	1.74	485.74

TABLE 8. Decision variables and calculating time for IEEE 118-bus system.

DR ratio = 0	Comparative method: current TR-TNEP	Proposed method: DAR-TNEP
First-stage variables	L_{1-2} / L_{8-9} / L_{9-10} / L_{12-117} / L_{24-72} / L_{32-114} / L_{68-116} / L_{71-72} / L_{77-78} = 1, L_{23-24} = 2, L_{71-73} = 3, L_{70-71} = 4	L_{1-2} / L_{8-9} / L_{9-10} / L_{12-117} / L_{32-114} / L_{68-116} / L_{77-78} = 1
The worst scenario (MW)	P_{R71} = 391MW P_{R10} = 96MW	P_{R71} = 0MW P_{R73} = 535MW P_{R10} = 96MW
Calculating time(s)	30069	21731

TABLE 9. Extreme scenarios of wind power output obtained by TR-TNEP for IEEE 118-bus system.

Method	TR-TNEP			
Extreme scenario	ES1	ES2	ES3	ES4
P_{R2} (MW)	31.17	31.17	322.66	322.66
P_{R3} (MW)	33.14	307.41	307.41	33.14

TABLE 10. Extreme scenarios of wind power output obtained by TR-TNEP for Garver 6-bus system.

Method	DAR-TNEP			
Extreme scenario	ES1	ES2	ES3	ES4
P_{R2} (MW)	128.33	31.17	219.41	322.66
P_{R3} (MW)	124.56	307.41	221.60	33.14

4) COST-EFFECTIVENESS ANALYSIS FOR DR PROGRAM

To analysis the benefits from DR programs quantitatively, the line investment saved by unit DR is introduced and denoted by $COST_{DR}^{k}$ when the DR ratio is k. The index is

TABLE 11. Extreme scenarios of wind power output obtained by DAR-TNEP for Garver 6-bus system.

Method	TR-TNEP							
Extreme scenario	ES1	ES2	ES3	ES4	ES5	ES6	ES7	ES8
P_{R71} (MW)	0	0	0	0	391.03	391.03	391.03	391.03
P_{R10} (MW)	0	0	96.29	96.29	0	0	96.29	96.29
P_{R72} (MW)	0	534.60	0	534.60	0	534.60	0	534.60

defined as (36):

$$COST_{DR}^{k} = \frac{COST_{line}^{0} - COST_{line}^{k}}{k^{*}sum(P_{Di})} \tag{30}$$

where $COST_{line}^{k}$ is the line investment when the DR ratio is k and $k^{*}sum\,(P_{Di})$ represents the maximal available DR resource. The index is calculated with the statistics in TABLE 1 and TABLE 4, the result is shown in TABLE 5.

Compared to the current DR cost of $0.034{*}10^{6}$ \$/MW in China, the profit gained by DR is much more considerable. As the line installation cost increases, the benefit of taking DR as an alternative will be more remarkable, considering the lower DR cost owing to the development of DR mechanism.

B. IEEE 118-BUS SYSTEM

For a modified IEEE 118-bus system, three wind farms are installed at Bus 10, Bus 71 and Bus 73 with the extreme output generated by TR-TNEP or DAR-TNEP (shown in TABLE 11 or TABLE 12 in Appendix). The DR ratios are assumed as 0, 10% and 20%. The cost of TR-TNEP case or DAR-TNEP case is given in TABLE 6 or TABLE 7, respectively.

It can be seen that the cost obtained by DAR-TNEP method almost has a 40% decrease compared to that of TR-TNEP.

C. VALIDATION OF THE PROPOSED DAR-TNEP

The superiority of DAR-TNEP in conservativeness and calculating efficiency compared with TR-TNEP is indicated in TABLE 8. The variable L_{i-j} denotes the number of the newly-installed circuit between Bus i and Bus j.

Fewer line investment is needed to relieve all the overflow for DAR-TNEP, which means the decision made by TR-TNEP is over-conservative. In addition, the calculating process is markedly accelerated when applying DAR-TNEP.

V. CONCLUSION

In this paper, the data adaptive robust transmission network expansion planning incorporating post-contingency demand response is proposed. By utilizing the correlation observed from historical data, the proposed DAR-TNEP overcomes the disadvantage of traditional TNEP using robust optimization. The conservativeness of the decisions is reduced. The combination of scenario-generation approach and robust optimization enables the proposed model to achieve both simplicity and robustness. The demand response alleviates the contingency overflow in multiple scenarios, thereby DR reduces the need for expansion while the reliability of system operation is not compromised. Case studies indicate that despite not every penny invested in DR makes a reduction in expansion cost, the trade-off between DR and line investment can be optimized via the carefully chosen DR ratio.

TABLE 12. Extreme scenarios of wind power output obtained by DAR-TNEP for IEEE 118-bus system.

Method	DAR-TNEP					
Extreme scenario	ES1	ES2	ES3	ES4	ES5	ES6
P_{R71} (MW)	391.03	130.34	296.70	166.70	260.30	0
P_{R10} (MW)	0	64.20	23.20	17.90	69.50	96.29
P_{R72} (MW)	0	178.20	307.40	242.80	242.80	534.60

APPENDIX

See Tables 9–12.

REFERENCES

[1] Y. Zhang, X. Wang, W. Zhang, F. Hou, and Z. Wu, "Analysis of technical strategies towards a low carbon electricity system in Europe," in *Proc. Int. Conf. Electr. Utility Deregulations Restruct. Power Technol.*, Nov. 2015, pp. 2561–2565.

[2] Z. Hungerford, A. Bruce, and I. MacGill, "Review of demand side management modelling for application to renewables integration in Australian power markets," in *Proc. IEEE PES Asia–Pacific Power Energy Eng. Conf.*, Nov. 2016, pp. 1–5.

[3] S. Mukhopadhyay, "Indian experience of smart grid applications in transmission and distribution system," in *Proc. IEEE Power India Int. Conf.*, Dec. 2015, pp. 1–6.

[4] W. Li, P. Xu, X. Lu, H. Wang, and Z. Pang, "Electricity demand response in China: Status, feasible market schemes and pilots," *Energy*, vol. 114, pp. 981–994, Nov. 2016.

[5] J. Dong, G. Xue, and R. Li, "Demand response in China: Regulations, pilot projects and recommendations—A review," *Renew. Sustain. Energy Rev.*, vol. 59, pp. 13–27, Jun. 2016.

[6] J. Ning, Y. Tang, and B. Gao, "A time-varying potential-based demand response method for mitigating the impacts of wind power forecasting errors," *Appl. Sci.*, vol. 7, no. 11, p. 1132, 2017.

[7] X. Han, M. Zhou, G. Li, and K. Y. Lee, "Stochastic unit commitment of wind-integrated power system considering air-conditioning loads for demand response," *Appl. Sci.*, vol. 7, no. 11, p. 1154, 2017.

[8] D. Koolen, N. Sadat-Razavi, and W. Ketter, "Machine learning for identifying demand patterns of home energy management systems with dynamic electricity pricing," *Appl. Sci.*, vol. 7, no. 11, p. 1160, 2017.

[9] S. Fan, G. He, K. Jia, and Z. Wang, "A novel distributed large-scale demand response scheme in high proportion renewable energy sources integration power systems," *Appl. Sci.*, vol. 8, no. 3, p. 452, 2018.

[10] C. Li, Z. Dong, G. Chen, F. Luo, and J. Liu, "Flexible transmission expansion planning associated with large-scale wind farms integration considering demand response," *IET Gener. Transmiss. Distrib.*, vol. 9, no. 15, pp. 2276–2283, 2015.

[11] A. Hajebrahimi, A. Abdollahi, and M. Rashidinejad "Probabilistic multiobjective transmission expansion planning incorporating demand response resources and large-scale distant wind farms," *IEEE Syst. J.*, vol. 11, no. 2, pp. 1170–1181, Jun. 2017.

[12] N. Zhang, Z. Hu, C. Springer, Y. Li, and B. Shen, "A bi-level integrated generation-transmission planning model incorporating the impacts of demand response by operation simulation," *Energy Convers. Manage.*, vol. 123, pp. 84–94, Sep. 2016.

[13] Ö. Özdemir, F. D. Munoz, J. L. Ho, and B. F. Hobbs, "Economic analysis of transmission expansion planning with price-responsive demand and quadratic losses by successive LP," *IEEE Trans. Power Syst.*, vol. 31, no. 2, pp. 1096–1107, Mar. 2016.

[14] X. Ai, J. Li, J. Fang, W. Yao, H. Xie, R. Cai, and J. Wen, "Multi-time-scale coordinated ramp-rate control for photovoltaic plants and battery energy storage," *IET Renew. Power Gener.*, vol. 12, no. 12, pp. 1390–1397, 2018.

[15] W. Gan, X. Ai, J. Fang, M. Yan, W. Yao, W. Zuo, and J. Wen, "Security constrained co-planning of transmission expansion and energy storage," *Appl. Energy*, vol. 239, pp. 383–394, Aug. 2019.

[16] H. Shuai, J. Fang, X. Ai, J. Wen, and H. He, "Optimal real-time operation strategy for microgrid: An ADP-based stochastic nonlinear optimization approach," *IEEE Trans. Sustain. Energy*, vol. 10, no. 2, pp. 931–942, Apr. 2019.

[17] J. Fang, Q. Zeng, X. Ai, Z. Chen, and J. Wen, "Dynamic optimal energy flow in the integrated natural gas and electrical power systems," *IEEE Trans. Sustain. Energy*, vol. 9, no. 1, pp. 188–198, Jan. 2018.

[18] S. M. Ryan, J. D. McCalley and D. L. Woodruff. (2011). *Long Term Resource Planning for Electric Power Systems Under Uncertainty*. [Online] Available: http://works.bepress.com/sarah_m_ryan/27/

[19] R. A. Jabr, "Robust transmission network expansion planning with uncertain renewable generation and loads," *IEEE Trans. Power Syst.*, vol. 28, no. 4, pp. 4558–4567, Nov. 2013.

[20] B. Chen, J. Wang, L. Wang, Y. He, and Z. Wang, "Robust optimization for transmission expansion planning: Minimax cost vs. minimax regret," *IEEE Trans. Power Syst.*, vol. 29, no. 6, pp. 3069–3077, Nov. 2014.

[21] S. Dehghan and N. Amjady, "Robust transmission and energy storage expansion planning in wind farm-integrated power systems considering transmission switching," *IEEE Trans. Sustain. Energy*, vol. 7, no. 2, pp. 765–774, Apr. 2016.

[22] L. Baringo and A. Baringo, "A stochastic adaptive robust optimization approach for the generation and transmission expansion planning," *IEEE Trans. Power Syst.*, vol. 33, no. 1, pp. 792–802, Jan. 2018.

[23] R. García-Bertrand and R. Mínguez, "Dynamic robust transmission expansion planning," *IEEE Trans. Power Syst.*, vol. 32, no. 4, pp. 2618–2628, Jul. 2017.

[24] C. Zhao, J. Wang, J.-P. Watson, and Y. Guan, "Multi-stage robust unit commitment considering wind and demand response uncertainties," *IEEE Trans. Power Syst.*, vol. 28, no. 3, pp. 2708–2717, Aug. 2013.

[25] R. Jiang, J. Wang, and Y. Guan, "Robust unit commitment with wind power and pumped storage hydro," *IEEE Trans. Power Syst.*, vol. 27, no. 2, pp. 800–810, May 2012.

[26] D. Bertsimas, E. Litvinov, X. A. Sun, J. Zhao, and T. Zheng, "Adaptive robust optimization for the security constrained unit commitment problem," *IEEE Trans. Power Syst.*, vol. 28, no. 1, pp. 52–63, Feb. 2013.

[27] C. Zhao and Y. Guan, "Unified stochastic and robust unit commitment," *IEEE Trans. Power Syst.*, vol. 28, no. 3, pp. 3353–3361, Aug. 2013.

[28] Y. Dvorkin, H. Pandzic, M. A. Ortega-Vazquez, and D. S. Kirschen, "A hybrid stochastic/interval approach to transmission-constrained unit commitment," *IEEE Trans. Power Syst.*, vol. 30, no. 2, pp. 621–631, Mar. 2015.

[29] H. Pandzic, Y. Dvorkin, T. Qiu, Y. Wang, and D. Kirschen, "Toward cost-efficient and reliable unit commitment under uncertainty," in *Proc. IEEE Power Energy Soc. General Meeting*, Jul. 2016, p. 1.

[30] Y. Zhang, S. Shen, and J. L. Mathieu, "Distributionally robust chance-constrained optimal power flow with uncertain renewables and uncertain reserves provided by loads," *IEEE Trans. Power Syst.*, vol. 32, no. 2, pp. 1378–1388, Mar. 2017.

[31] Y. Guan and J. Wang, "Uncertainty sets for robust unit commitment," *IEEE Trans. Power Syst.*, vol. 29, no. 3, pp. 1439–1440, May 2014.

[32] P. Kumar and E. A. Yildirim, "Minimum-volume enclosing ellipsoids and core sets," *J. Optim. Theory Appl.*, vol. 126, no. 1, pp. 1–21, 2005.

[33] X. Xu, X. He, Q. Ai, and R. C. Qiu, "A correlation analysis method for power systems based on random matrix theory," *IEEE Trans. Smart Grid*, vol. 8, no. 4, pp. 1811–1820, Jul. 2017.

[34] W. Wei, F. Liu, and S. Mei, "Distributionally robust co-optimization of energy and reserve dispatch," *IEEE Trans. Sustain. Energy*, vol. 7, no. 1, pp. 289–300, Jan. 2017.

[35] C. Zhao and Y. Guan, "Data-driven stochastic unit commitment for integrating wind generation," *IEEE Trans. Power Syst.*, vol. 31, no. 4, pp. 2587–2596, Jul. 2016.

[36] Y. Zhang, X. Ai, J. Wen, J. Fang, and H. He, "Data-adaptive robust optimization method for the economic dispatch of active distribution networks," *IEEE Trans. Smart Grid*, vol. 10, no. 4, pp. 3791–3800, Jul. 2019.

QIANWEI ZHENG received the B.S. degree in electrical engineering from the Huazhong University of Science and Technology (HUST), Wuhan, China, in 2017, where she is currently pursuing the M.S. degree with the School of Electrical and Electronics Engineering. Her current research interests include transmission network planning and renewable energy integration.

XIAOMENG AI (S'11–M'17) received the B.Eng. degree in mathematics and applied mathematics and the Ph.D. degree in electrical engineering from the Huazhong University of Science and Technology (HUST), Wuhan, China, in 2008 and 2014, respectively, where he is currently a Lecturer. His research interests include robust optimization, stochastic optimization, renewable energy integration, and integrated energy market.

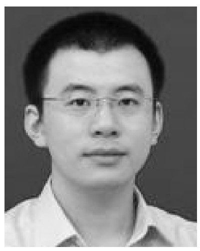

JIAKUN FANG (S'10–M'13–SM'19) received the B.Sc. and Ph.D. degrees from the Huazhong University of Science and Technology (HUST), Wuhan, China, in 2007 and 2012, respectively, he is currently a Full Professor. He held a Postdoctoral position at the Department of Energy Technology, Aalborg University, Aalborg, Denmark, in 2012, where he was an Assistant Professor, in 2015, and an Associate Professor, in 2018. His research interests include power system dynamic stability control, power grid complexity analysis, and integrated energy systems.

JINYU WEN (M'10) received the B.S. and Ph.D. degrees in electrical engineering from the Huazhong University of Science and Technology (HUST), Wuhan, China, in 1992 and 1998, respectively.

He was a Visiting Student, from 1996 to 1997, and Research Fellow, from 2002 to 2003, with the University of Liverpool, Liverpool, U.K., and a Senior Visiting Researcher with The University of Texas at Arlington, Arlington, TX, USA, in 2010. From 1998 to 2002, he was a Director Engineer with XJ Electric Company Ltd., China. In 2003, he joined HUST, where he is currently a Professor with the School of Electrical and Electronics Engineering. His current research interests include renewable energy integration, energy storage, multi-terminal HVDC, and power system operation and control.